Magnetocaloric effects in *R*NiIn (*R* = Gd-Er) intermetallic compounds

H. Zhang,[1,a)] Z. Y. Xu,[1] X. Q. Zheng,[1] J. Shen,[2] F. X. Hu,[1] J. R. Sun[1], and B. G. Shen[1]
[1]*State Key Laboratory for Magnetism, Institute of Physics, Chinese Academy of Sciences, Beijing, 100190, People's Republic of China*
[2]*Key laboratory of Cryogenics, Technical Institute of Physics and Chemistry, Chinese Academy of Sciences, Beijing, 100190, People's Republic of China*

(Received 7 April 2011; accepted 19 May 2011; published online 28 June 2011)

Magnetic properties and magnetocaloric effects (MCEs) of the intermetallic *R*NiIn (*R* = Gd-Er) compounds have been investigated in detail. GdNiIn and ErNiIn compounds exhibit a ferromagnetic (FM) to paramagnetic (PM) transition around the respective Curie temperatures. However, it is found that *R*NiIn with *R* = Tb, Dy, and Ho undergo two successive magnetic phase transitions with increasing temperature. In addition, a field-induced metamagnetic transition from antiferromagnetic (AFM) to FM states is observed in *R*NiIn with *R* = Tb and Dy below their respective AFM-FM transition temperatures (T_t). The maximal values of magnetic entropy change (ΔS_M) of HoNiIn are –9.5 J/kg K at $T_t = 7$ K and –21.7 J/kg K at $T_C = 20$ K for a magnetic field change of 5 T, respectively. These two successive ΔS_M peaks overlap partly, giving rise to a high value of refrigerant capacity (*RC* = 341 J/kg at 5 T) over a wide temperature span. It is noted that the *RC* value of GdNiIn is as high as 326 J/kg due to the relatively broad distribution of ΔS_M peak. Consequently, this *R*NiIn system shows large reversible ΔS_M and considerable *RC* values in the temperature range of 10–100 K. © *2011 American Institute of Physics*. [doi:10.1063/1.3603044]

I. INTRODUCTION

Recently, magnetic refrigeration based on the magnetocaloric effect (MCE) is expected to be a potential technique due to its energy efficiency and environment safety in comparison with the conventional gas compression-expansion technique.[1–6] To improve the application of magnetic refrigerant technology, many efforts have been made to explore advanced magnetocaloric materials. So far, numerous materials with the first-order magnetic or structural phase transition, such as $Gd_5(Si_{1-x}Ge_x)_4$,[7,8] La(Fe, X)$_{13}$ (X = Si, Al),[9–11] MnAs,[12] MnFe(P, As),[13] $ErCo_2$,[14] and Heusler alloys,[15,16] etc., have been found to exhibit giant MCEs around their transition temperatures. However, the remarkable thermal and magnetic hystereses, accompanied with the first-order phase transition, always reduce the actual efficiencies of these materials in the cooling cycles. Therefore, it is necessary to search for magnetic materials with large reversible MCEs and refrigerant capacity (*RC*) based on the second-order magnetic transition.

From the viewpoint of practical applications, the rare earth (*R*)-based intermetallic compounds exhibiting large MCEs at lower temperatures are potential magnetic refrigerants for the gas liquefiers. In order to obtain a large MCE, much attention has been paid to the *R*-based intermetallic compounds with low-temperature phase transition. Some *R*-based compounds with a second-order magnetic transition, such as *R*CoAl,[17] *R*CuSi,[18,19] *R*CuAl,[20] and R_2In,[21,22] have been reported to possess not only large magnetic entropy change (ΔS_M) and/or adiabatic temperature change (ΔT_{ad}) but also a small hysteresis loss in a wide temperature region.

The ternary intermetallic *R*NiIn compounds, which crystallize in the ZrNiAl-type hexagonal structure with space group $P\bar{6}2m$, have been investigated extensively in the past few decades due to interesting physical properties.[23–27] The magnetic studies revealed that these compounds show ferromagnetic (FM) behavior with the magnetic ordering temperature changing from 96 K for *R* = Gd to 9 K for *R* = Er.[28,29] In addition, the neutron diffraction studies have indicated that *R*NiIn (*R* = Gd, Ho, and Er) are predominantly FM, whereas DyNiIn exhibits an antiferromagnetic (AFM) ground state.[26,30,31] Meanwhile, the neutron diffraction data at 1.5 K for TbNiIn suggests a complex magnetic structure with the FM and AFM components.[28,30] Recently, Canepa *et al.*[32] reported the MCE in GdNiIn and the maximal values of ΔS_M and ΔT_{ad} are –6.7 J/kg K and 2.8 K for a field change of 0–5 T, respectively. However, a careful study on MCEs for this *R*NiIn system is still lacking and remains to be carried out. In the present paper, we study on the magnetic and magnetocaloric properties of *R*NiIn compounds with *R* = Gd-Er in detail. It has been found that the *R*NiIn compounds present large reversible MCEs and considerable *RC* in the temperature range of 10–100 K.

II. EXPERIMENTAL DETAILS

The polycrystalline *R*NiIn (*R* = Gd-Er) samples were prepared by arc-melting appropriate proportions of constituent components with the purity better than 99.9 wt. % on a water-cooled copper hearth under argon atmosphere. Each sample was melted several times with the button being turned over after each melting to ensure the homogeneity. The obtained ingots were then annealed in a high-vacuum quartz tube at 1073 K for 7–10 days. Powder X-ray diffraction (XRD) measurements were performed at room

a)Author to whom correspondence was addressed. Electronic mail: zhanghuxt@gmail.com.

 © 2011 American Institute of Physics

Author complimentary copy. Redistribution subject to AIP license or copyright, see http://jap.aip.org/jap/copyright.jsp

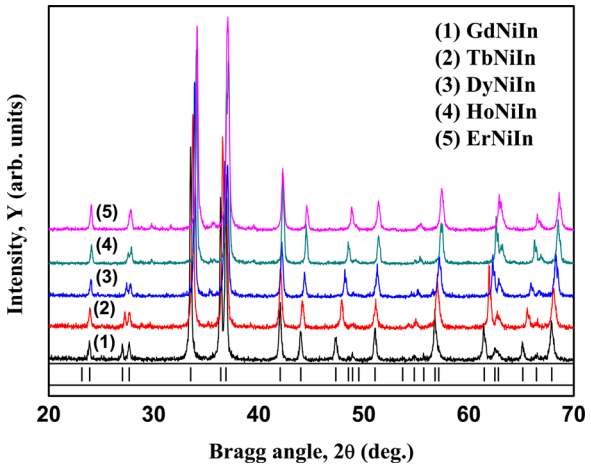

FIG. 1. (Color online) The X-ray diffraction patterns of *R*NiIn (*R* = Gd-Er) compounds at room temperature. The short vertical lines indicate the Bragg peak positions of the ZrNiAl-type hexagonal structure calculated from the Rietveld refinement based on the XRD pattern of GdNiIn.

temperature by using Cu Kα radiation to identify the crystal structure and the lattice parameters. Magnetizations were measured as functions of temperature and magnetic field by employing a commercial superconducting quantum interference device (SQUID) magnetometer, model MPMS-7 from Quantum Design Inc.

III. RESULTS AND DISCUSSION

The powder X-ray diffraction (XRD) patterns of the *R*NiIn (*R* = Gd-Er) compounds at room temperature are shown in Fig. 1(a). All samples crystallize in a single phase with the ZrNiAl-type hexagonal structure (space group $P\bar{6}2m$). It is clearly observed that the Bragg reflection shifts continuously to high angle with the rare-earth atom sweeping from Gd to Er, suggesting the lattice constants of *R*NiIn compounds decrease linearly due to the lanthanide contraction. The unit cell volumes and the densities were determined from the Rietveld refinement based on the XRD patterns, and their values are listed in Table I. The values of lattice parameter and unit cell volume in our study are in good agreement with the data in previous reports.[23,28]

The Curie temperature (T_C), which is defined as the minimum in the dM/dT versus T curve, decreases from 98 K for *R* = Gd to 9 K for *R* = Er. Above their respective ordering temperatures, the magnetic susceptibilities of all *R*NiIn compounds follow the Curie-Weiss law. The values of T_C, PM Curie temperature (θ_P), and the effective magnetic moment (μ_{eff}), calculated from the Curie-Weiss fits of reciprocal magnetic susceptibility χ_m^{-1} versus T curves, for the *R*NiIn compounds are summarized in Table I and are consistent with the values reported in Refs. 28 and 29.

Figure 2 shows the temperature (T) dependencies of zero-field-cooling (ZFC) and field-cooling (FC) magnetizations (M) under a magnetic field of 0.05 T for *R*NiIn compounds with *R* = Tb, Dy, and Ho. For all the compounds, no thermal hysteresis between ZFC and FC M-T curves around T_C is observed as shown usually in magnetic materials with second-order magnetic transition. However, it is found that there is a difference between ZFC and FC curves below T_C, and this irreversibility is likely related to the domain wall pinning effect. The neutron diffraction data at 1.5 K has indicated that DyNiIn exhibits an antiferromagnetic (AFM) ground state, while TbNiIn possesses a complex magnetic structure with the FM and AFM components at low temperature.[28,30,31] The M-T curves in Figs. 2(a1) and 2(b1) show that both TbNiIn and DyNiIn experience two magnetic transitions with the increase of temperature. The anomaly at lower temperature is probably associated with the phase transition from AFM to FM states, and the other abrupt change of magnetization around T_C corresponds to the magnetic transition from FM to PM states. The AFM-FM transition temperatures (T_t), derived from the dM/dT versus T curve, are about 12 and 14 K for TbNiIn and DyNiIn, respectively (the insets of Figs. 2(a1) and 2(b1)). The temperature dependencies of the magnetization of *R*NiIn with *R* = Tb and Dy were measured in various magnetic fields as shown in Figs. 2(a2) and 2(b2), respectively. It is observed that a field-induced metamagnetic transition from AFM to FM states occurs below T_t with increasing magnetic field. The stepwise behavior of the M-T curves around T_C under high magnetic fields corresponds to the FM to PM transition.

Figure 2(c1) shows that HoNiIn compound also exhibits two successive magnetic transitions with the increase of temperature. The first anomaly around T_t = 7 K, corresponding to the low-temperature peak in the dM/dT versus T curve (the inset of Fig. 2(c1)), is speculated to be a possible change from collinear to non-collinear magnetic structure. The second change of magnetization at T_C = 20 K is ascribed to the FM-PM transition. Figure 2(c2) presents the temperature dependencies of the magnetization of HoNiIn in various magnetic fields. The two magnetic transitions can be easily observed in

TABLE I. The crystallographic, magnetic, and magnetocaloric data for the *R*NiIn compounds with *R* = Gd-Er.

Compound	V (Å^3)	ρ (g/cm^3)	T_C (K)	T_t (K)	θ_P (K)	μ_{eff} (μ_B) Exp.	μ_{eff} (μ_B) Theor.	$-\Delta S_M$ (2 T) (J/kg K)	$-\Delta S_M$ (5 T) (J/kg K)	RC (5 T) (J/kg)
GdNiIn	183.8 (7)	8.786	98	–	101	7.96	7.94	3.3	7.1	326
TbNiIn	181.4 (5)	9.129	71	12	47	9.80	9.72	2.4	5.3	191
DyNiIn	179.4 (3)	9.325	30	14	31	10.68	10.63	5.5	10.4	270
HoNiIn	177.8 (1)	9.478	20	7	18	10.61	10.60	12.7	21.7	341
ErNiIn	176.3 (7)	9.696	9	–	8	9.64	9.59	10.1	15.1	229

Author complimentary copy. Redistribution subject to AIP license or copyright, see http://jap.aip.org/jap/copyright.jsp

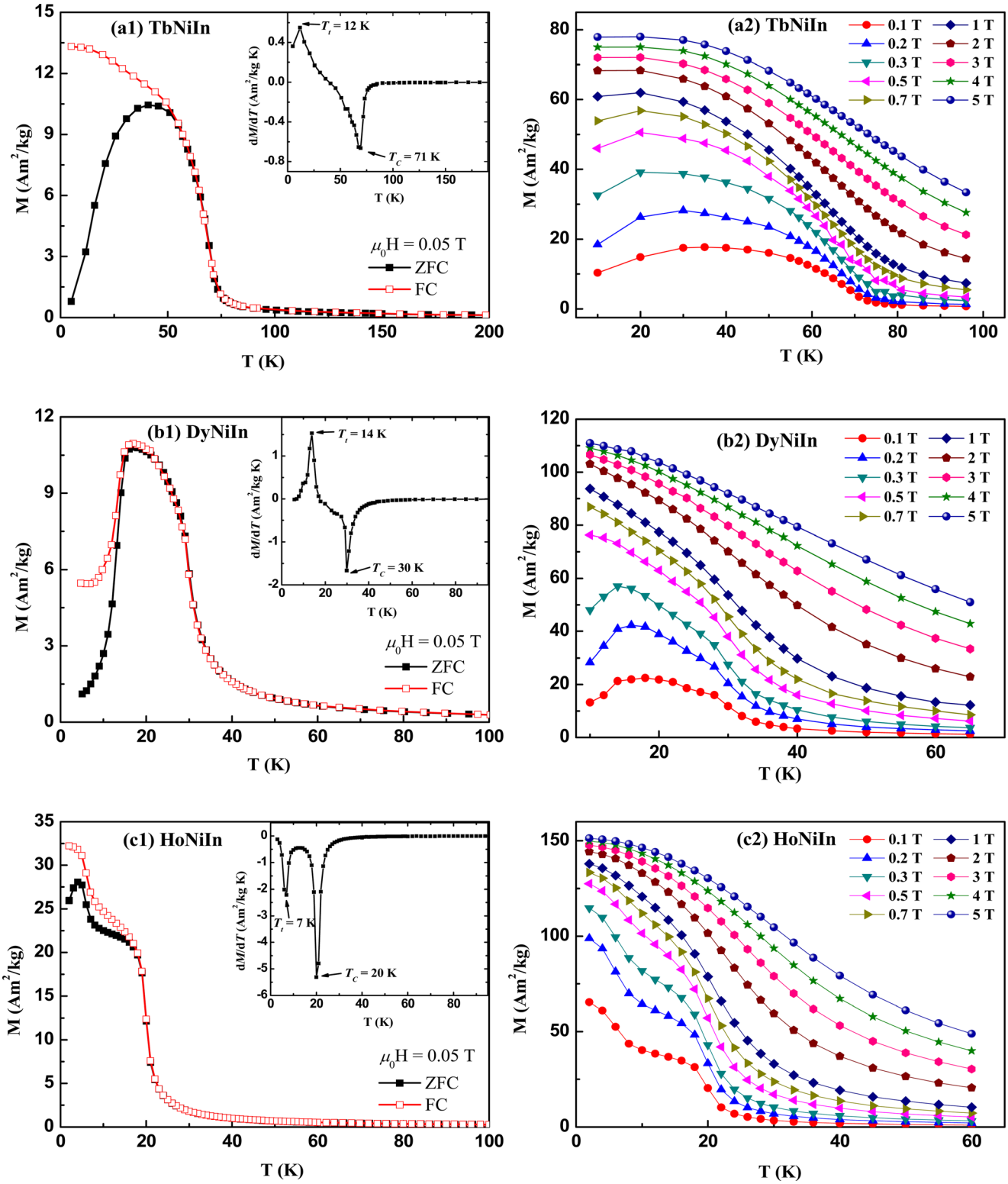

FIG. 2. (Color online) Temperature dependencies of the magnetization measured during ZFC (solid symbols) and FC (open symbols) cycles for *R*NiIn with *R* = (a1) Tb, (b1) Dy, and (c1) Ho under a magnetic field of 0.05 T, and the temperature dependencies of the magnetization in various magnetic fields for (a2) TbNiIn, (b2) DyNiIn, and (c2)HoNiIn, respectively. The insets show the d*M*/d*T*-*T* curves for these compounds.

the low field range. However, the transition around 7 K vanishes when the magnetic field is higher than 1 T.

Magnetization isotherms of these compounds were measured in a wide temperature range with different temperature steps under applied fields up to 5 T. It is found that all *R*NiIn compounds exhibit similar *M*-*H* curves around their respective Curie temperatures. Figure 3(a) shows the magnetization isotherms of HoNiIn. The magnetization increases sharply at low fields and shows a tendency to saturate with increasing the field, suggesting the typical FM behavior. In addition, each magnetization isotherm around T_C shows a completely reversible behavior during the field increasing

Author complimentary copy. Redistribution subject to AIP license or copyright, see http://jap.aip.org/jap/copyright.jsp

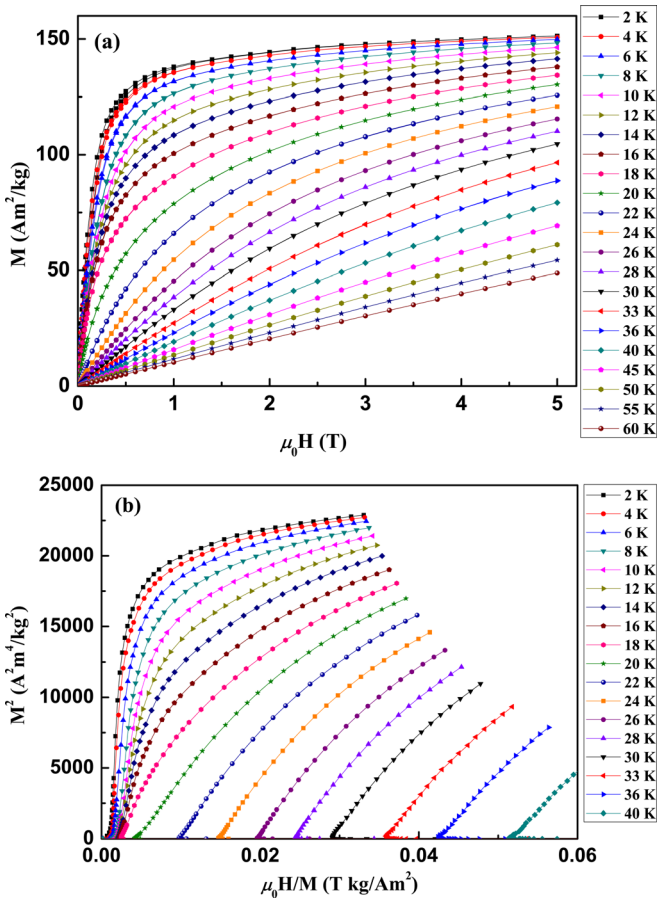

FIG. 3. (Color online) (a) Isothermal magnetization curves of HoNiIn compound in a temperature range of 2–60 K with field increasing and decreasing in different temperature steps, (b) and Arrott plots of HoNiIn in a temperature range of 2–40 K.

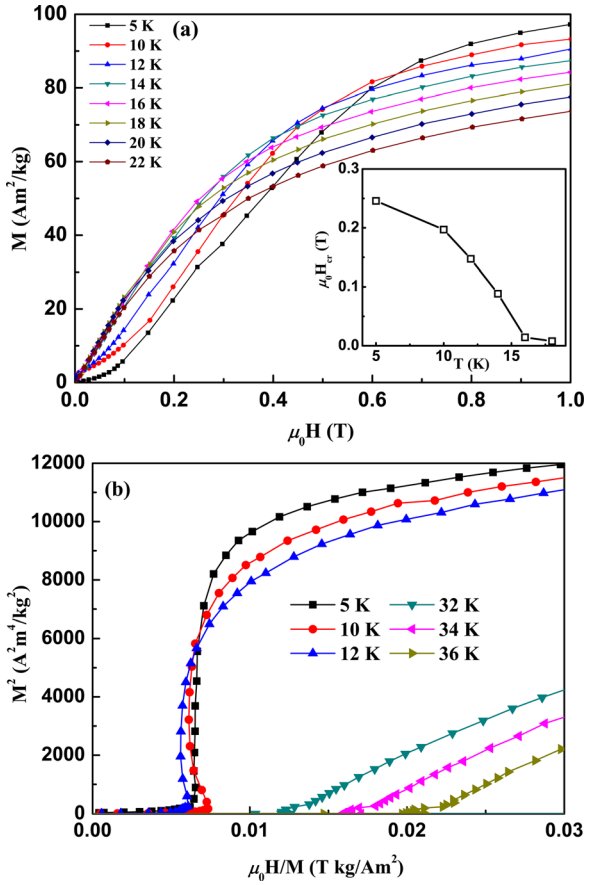

FIG. 4. (Color online) (a) Isothermal magnetizations of DyNiIn below T_C in a low magnetic field range of 0–1 T and the inset shows the temperature dependence of the critical magnetic field. (b) The Arrott plots of DyNiIn below the critical temperature T_t and just above T_C.

and decreasing cycles, which is favorable to practical applications of the magnetic refrigeration materials. The Arrott plots of HoNiIn in the temperature range of 2–40 K are shown in Fig. 3(b). As is well known, a magnetic transition is considered as first-order when the slope of Arrott plot is negative; whereas it is expected to be of second-order when the slope is positive.[33] There are neither inflection points nor negative slopes, proving that HoNiIn compounds exhibit a second-order FM-PM magnetic transition. Figure 4(a) displays the magnetization isotherms of DyNiIn below the ordering temperature in a low field region. It is observed that the magnetization of DyNiIn below 14 K increases linearly with the increase of magnetic field in low field range, suggesting the existence of AFM component at low temperatures.[31] However, the magnetization increases rapidly with increasing the magnetic field and saturates gradually under high applied field, confirming the field-induced metamagnetic transition from AFM to FM states. As shown in the inset of Fig. 4(a), the critical magnetic field required for metamagnetism, determined from the maximum of dM/dH curve, increases monotonically with the decrease of temperature and attains a value of 0.25 T at 5 K. This result illustrates that the AFM-FM metamagnetic transition can be induced easily by a relatively low filed. Figure 4(b) shows the Arrott plots of DyNiIn below the critical temperature T_t and just above T_C. It is found that the Arrott plots below T_t exhibit a negative slope, further confirming the first-order AFM-FM metamagnetic transition. However, the positive slope of the plots above T_C indicates the characteristic of the second-order FM-PM magnetic transition. Similar phenomenon of the AFM-FM metamagnetic transition was also observed in the case of TbNiIn.

In an isothermal process of magnetization, the ΔS_M of the materials can be derived from the Maxwell relation

$$\Delta S_M = \int_0^H (\partial M/\partial T)_H dH. \tag{1}$$

In practice, the ΔS_M usually can be calculated using the following alternative formula[15,34]

$$\Delta S_M = \sum_i \frac{M_{i+1} - M_i}{T_{i+1} - T_i} \Delta H_i, \tag{2}$$

where M_i and M_{i+1} are the magnetization values at temperatures T_i and T_{i+1} in a magnetic field H_i, respectively. The ΔS_M of RNiIn with R = Gd-Er associated with the field variation were calculated according to Eq. (2) and the maximal values of ΔS_M for the magnetic field changes of 0–2 T and 0–5 T are presented in Table I and Figs. 5(a) and 5(b), respectively. It is clearly seen from Fig. 5 that with the R element sweeping from Gd to Er, the Curie temperature of RNiIn decreases linearly, whereas the ΔS_M roughly increases

Author complimentary copy. Redistribution subject to AIP license or copyright, see http://jap.aip.org/jap/copyright.jsp

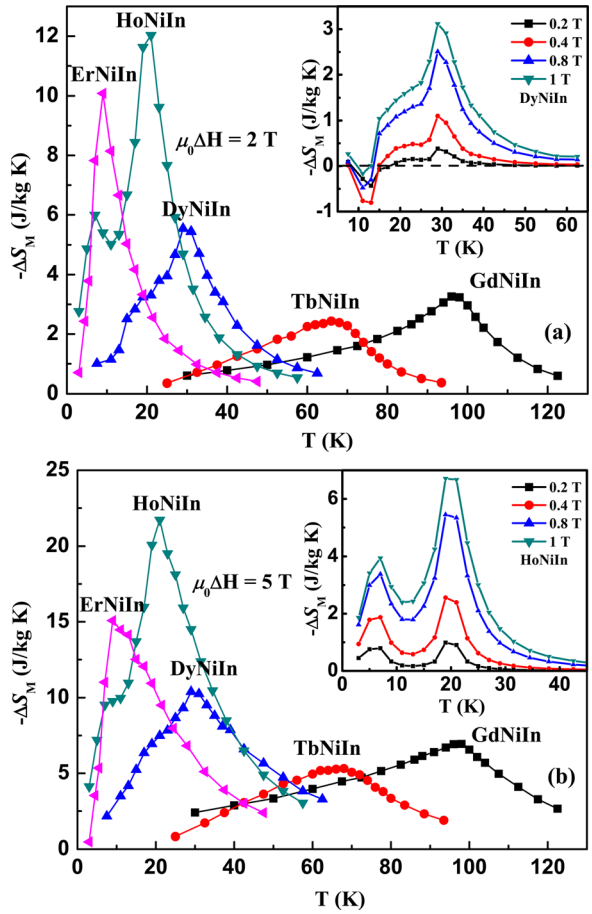

FIG. 5. (Color online) Temperature dependencies of the isothermal magnetic entropy changes ΔS_M for *R*NiIn (R = Gd-Er) compounds under magnetic field changes of (a) 0–2 T and (b) 0–5 T, respectively. The insets show the temperature dependencies of ΔS_M under the low magnetic field changes for DyNiIn and HoNiIn, respectively.

and reaches the highest value in HoNiIn compound. This tendency is similar to the results in other *R*-based intermetallic systems.[17] A small negative value of $-\Delta S_M$ for DyNiIn was observed below 14 K in low magnetic field range as shown in the inset of Fig. 5(a), but it gradually changes to positive value with the increase of magnetic field. Such a sign change of $-\Delta S_M$ is due to the field-induced magnetic transition from AFM to FM states. On the other hand, It is worthwhile to note that a large reversible $-\Delta S_M$ of 12.7 J/kg K for HoNiIn is obtained at T_C under a low field change of 0–2 T, which is beneficial to practical applications since a magnetic field of 2 T can be provided by a permanent magnet. Besides, another $-\Delta S_M$ peak as high as 6 and 9.5 J/kg K for the field changes of 0–2 T and 0–5 T is observed in HoNiIn at 7 K, corresponding to the low-temperature magnetic phase transition. It is noticed that the successive ΔS_M peaks can be clearly seen even under the low magnetic field changes (the inset of Fig. 5(b)), and thus obviously enlarging the temperature range of MCE.

The *RC* value is another important parameter to quantify amount of heat transferred during an ideal refrigeration cycle. The *RC* values of *R*NiIn are estimated according to the approach suggested by Gschneidner *et al.*,[35] namely, $RC = \int_{T_1}^{T_2} |\Delta S_M| dT$, where T_1 and T_2 are the temperatures corresponding to both ends of the half-maximum value of ΔS_M peak, respectively. To obtain the effective *RC* value, it is necessary to take into account the hysteresis loss since that will make magnetic refrigeration less efficient. However, no magnetic hysteresis is observed for all the investigated samples around their respective T_C, suggesting a perfectly reversible MCE of these compounds for practical applications. The *RC* values thus obtained are listed in Table I. It is found that the *R*NiIn compounds with R = Gd-Er show considerable values of *RC* over a wide temperature range of 10–100 K. Although the ΔS_M of GdNiIn is much smaller than that of HoNiIn, the *RC* value of GdNiIn is as high as 326 J/kg due to the relatively broad distribution of ΔS_M peak and its full width at half maximum of the ΔS_M peak is observed to be 64 K. In addition, HoNiIn exhibits the highest *RC* value of 341 J/kg for a field change of 0–5 T, which is much larger than those of some magnetic refrigerant materials in the similar magnetic transition temperatures, such as $GdPd_2Si$ (240 J/kg at 17 K),[36] and Tb_2PdSi_3 (245 J/kg at 23 K),[37] where the *RC* values are estimated from the ΔS_M versus T curves in literatures, respectively. The large *RC* originates from the combined contribution of two successive magnetic transitions, which enlarge the temperature span of large MCE.

IV. CONCLUSIONS

In conclusion, single-phase *R*NiIn (R = Gd-Er) compounds with the ZrNiAl-type hexagonal structure have been prepared and the magnetic and magnetocaloric properties of this system have been studied experimentally. All *R*NiIn compounds possess a second-order FM-PM transition around their respective Curie temperatures, which are consistent with previous studies. In addition, our results reveal that with the increase of temperature *R*NiIn with R = Tb and Dy exhibit a magnetic transition from AFM to FM states below T_C; while HoNiIn undergoes a magnetic transition around 7 K which may be associated with a possible change from collinear to non-collinear magnetic structure. The calculation of magnetic entropy change shows that all *R*NiIn compounds, especially HoNiIn, exhibit large MCEs around their respective T_C. A sign change of MCE is observed in DyNiIn below 14 K due to the field-induced magnetic transition from AFM to FM states. For a magnetic field change of 0–5 T, HoNiIn shows the highest values of $-\Delta S_M$ (21.7 J/kg K at T_C) and *RC* (341 J/kg) over a wide temperature range, which results from the combined contribution of the two successive transitions. In a word, the large reversible $-\Delta S_M$ as well as comparable *RC* values indicate that this series of *R*NiIn compounds could be promising candidates for magnetic refrigeration in the temperature range of 10–100 K.

ACKNOWLEDGMENTS

This work was supported by the National Natural Science Foundation of China, the Knowledge Innovation Project of the Chinese Academy of Sciences, the Hi-Tech Research and Development program of China, and China Postdoctoral Science Foundation Funded Project.

Author complimentary copy. Redistribution subject to AIP license or copyright, see http://jap.aip.org/jap/copyright.jsp

[1]C. B. Zimm, A. Jastrab, A. Sternberg, V. K. Pecharsky, K. A. Gschneidner Jr., M. Osborne, and I. Anderson, Adv. Cryog. Eng. **43**, 1759 (1998).
[2]V. K. Pecharsky and K. A. Gschneidner Jr., J. Magn. Magn. Mater. **200**, 44 (1999).
[3]K. A. Gschneidner Jr., V. K. Pecharsky, and A. O. Tsokol, Rep. Prog. Phys. **68**, 1479 (2005).
[4]A. M. Tishin, J. Magn. Magn. Mater. **316**, 351 (2007).
[5]E. Brück, O. Tegus, D. T. C. Thanh, and K. H. J. Buschow, J. Magn. Magn. Mater. **310**, 2793 (2007).
[6]B. G. Shen, J. R. Sun, F. X. Hu, H. W. Zhang, and Z. H. Cheng, Adv. Mater. **21**, 4545 (2009).
[7]V. K. Pecharsky and K. A. Gschneidner Jr., Phys. Rev. Lett. **78**, 4494 (1997).
[8]V. K. Pecharsky, A. P. Holm, K. A. Gschneidner Jr., and R. Rink, Phys. Rev. Lett. **91**, 197204 (2003).
[9]F. X. Hu, B. G. Shen, J. R. Sun, Z. H. Cheng, G. H. Rao, and X. X. Zhang, Appl. Phys. Lett. **78**, 3675 (2001).
[10]F. X. Hu, B. G. Shen, J. R. Sun, and Z. H. Cheng, Phys. Rev. B **64**, 012409 (2001).
[11]H. Zhang, Y. Long, Q. Cao, Y. Mudryk, M. Zou, K. A. Gschneidner Jr., and V. K. Pecharsky, J. Magn. Magn. Mater. **322**, 1710 (2010).
[12]H. Wada and Y. Tanabe, Appl. Phys. Lett. **79**, 3302 (2001).
[13]O. Tegus, E. Brück, K. H. J. Buschow, and F. R. de Boer, Nature (London) **415**, 150 (2002).
[14]A. Giguere, M. Foldeaki, W. Schnelle, and E. Gmelin, J. Phys.: Condens. Matter. **11**, 6969 (1999).
[15]F. X. Hu, J. R. Sun, G. H. Wu, and B. G. Shen, J. Appl. Phys. **90**, 5216 (2001).
[16]S. Y. Yu, Z. X. Cao, L. Ma, G. D. Liu, J. L. Chen, G. H. Wu, B. Zhang, and X. X. Zhang, Appl. Phys. Lett. **91**, 102507 (2007).
[17]X. X. Zhang, F. W. Wang, and G. H. Wen, J. Phys.: Condens. Matter. **13**, L747 (2001).
[18]J. Chen, B. G. Shen, Q. Y. Dong, and J. R. Sun, Solid State Commun. **150**, 1429 (2010).
[19]J. Chen, B. G. Shen, Q. Y. Dong, F. X. Hu, and J. R. Sun, Appl. Phys. Lett. **96**, 152501 (2010).
[20]Q. Y. Dong, B. G. Shen, J. Chen, J. Shen, and J. R. Sun, J. Appl. Phys. **105**, 113902 (2009).
[21]A. Bhattacharyya, S. Chatterjee, S. Giri, and S. Majumdar, J. Magn. Magn. Mater. **321**, 1828 (2009).
[22]H. Zhang, B. G. Shen, Z. Y. Xu, J. Chen, J. Shen, F. X. Hu, and J. R. Sun, J. Alloys Compd. **509**, 2602 (2011).
[23]R. Ferro, R. Marazza, and G. Rambaldi, Z. Metallkd. **65**, 37 (1974).
[24]K. H. J. Buschow, J. Less-Common Met. **39**, 185 (1975).
[25]F. Merlo, M. L. Fornasini, S. Cirafici, and F. Canepa, J. Alloys Compd. **267**, L12 (1998).
[26]L. Gondek, A. Szytula, B. Penc, J. Hernandez-Velasco, and A. Zygmunt, J. Magn. Magn. Mater. **262**, L177 (2003).
[27]J. Kaštil, P. Javorský, and M. Klicpera, Acta Phys. Pol., A **118**, 888 (2010).
[28] Yu. B. Tyvanchuk, Y. M. Kalyczak, L. Gondek, M. Rams, A. Szytula, and Z. Tomkowicz, J. Magn. Magn. Mater. **277**, 368 (2004).
[29]A. W. Carbonari, A. L. Lapolli, R. N. Saxena, and J. Mestnik-Filho, Hyperfine Interact. **176**, 101 (2007).
[30]L. Gondek, A. Szytula, S. Baran, and J. Hernandez-Velasco, J. Magn. Magn. Mater. **272–276** E443 (2004).
[31]L. Gondek, A. Szytula, S. Baran, M. Rams, J. Hernandez-Velasco, and Yu. Tyvanchuk, J. Magn. Magn. Mater. **278**, 392 (2004).
[32]F. Canepa, M. Napoletano, A. Palenzona, F. Merlo, and S. Cirafici, J. Phys. D Appl. Phys. **32**, 2721 (1999).
[33]S. K. Banerjee, Phys. Lett. **12**, 16 (1964).
[34]R. D. Mcmichael, J. J. Ritter, and R. D. Shull, J. Appl. Phys. **73**, 6946 (1993).
[35]K. A. Gschneidner Jr., V. K. Pecharsky, A. O. Pecharsky, and C. B. Zimm, Mater. Sci. Forum. **315–317** 69 (1999).
[36]R. Rawat and I. Das, J. Phys.: Condens. Matter **13**, L57 (2001).
[37]S. Majumdar, E. V. Sampathkumaran, P. L. Paulose, H. Bitterlich, W. Loser, and G. Behr, Phys. Rev. B **62**, 14207 (2000).

Author complimentary copy. Redistribution subject to AIP license or copyright, see http://jap.aip.org/jap/copyright.jsp